12-8-2022

# Genetic Expression Changes and Pathologic Findings Associated with Hyperhomocysteinemia in Human Autopsy Brain Tissue

Erica M. Weekman
*University of Kentucky*

Zachary Winder
*University of Kentucky*

Colin B. Rogers
*University of Kentucky*

Erin L. Abner
*University of Kentucky*

Tiffany L. Sudduth
*University of Kentucky*

## Repository Citation

# Genetic Expression Changes and Pathologic Findings Associated with Hyperhomocysteinemia in Human Autopsy Brain Tissue

## Digital Object Identifier (DOI)

https://doi.org/10.1002/trc2.12368

## Authors

Erica M. Weekman, Zachary Winder, Colin B. Rogers, Erin L. Abner, Tiffany L. Sudduth, Ela Patel, Adam J. Dugan, Shuling X. Fister, Brandi Wasek, Peter T. Nelson, Gregory A. Jicha, Teodoro Bottiglieri, David W. Fardo, and Donna M. Wilcock

RESEARCH ARTICLE

Alzheimer's & Dementia
Translational Research
& Clinical Interventions

# Genetic expression changes and pathologic findings associated with hyperhomocysteinemia in human autopsy brain tissue

Erica M. Weekman[1] | Zach Winder[1] | Colin B. Rogers[1] | Erin L. Abner[1] |
Tiffany L. Sudduth[1] | Ela Patel[1] | Adam J. Dugan[1] | Shuling X. Fister[1] |
Brandi Wasek[2] | Peter T. Nelson[1] | Gregory A. Jicha[1] | Teodoro Bottiglieri[2] |
David W. Fardo[1] | Donna M. Wilcock[1]

[1]Sanders-Brown Center on Aging, University of Kentucky, Lexington, Kentucky, USA

[2]Baylor Scott and White Research Institute, Center of Metabolomics, Institute of Metabolic Disease, Dallas, Texas, USA

**Correspondence**
Erica M. Weekman, Sanders-Brown Center on Aging, University of Kentucky, 789 S Limestone St, Rm 581, Lexington, KY 40536, USA.
E-mail: emweek2@uky.edu

## Abstract

**Introduction:** Vascular contributions to cognitive impairment and dementia (VCID) are a leading cause of dementia. An underappreciated, modifiable risk factor for VCID is hyperhomocysteinemia (HHcy), defined by elevated levels of plasma homocysteine, most often due to impaired B vitamin absorption in aged persons. Studies aimed at identifying neuropathologic features and gene expression profiles associated with HHcy have been lacking.

**Methods:** A subset of research volunteers from the University of Kentucky Alzheimer's Disease Research Center longitudinal cohort came to autopsy and had *ante mortem* plasma homocysteine levels available. Brain tissue and blood plasma drawn closest to death were used to measure homocysteine and related metabolites in the current pilot study. Genetic expression profiles of inflammatory markers were evaluated using the Human Neuroinflammation NanoString panel. Further analyses included an evaluation of plasma homocysteine effects on amyloid beta, tau, ionized calcium-binding adaptor molecule 1, and glial fibrillary acidic protein immunohistochemistry in the frontal and occipital cortices. Analytes and other study outcomes were evaluated in relation to *ante mortem* HHcy status: We identified 13 persons with normal *ante mortem* plasma homocysteine levels (<14 μmol/L) and 18 who had high plasma homocysteine levels (≥14 μmol/L).

**Results:** Participants with HHcy demonstrated increased levels of several plasma homocysteine cycle metabolites such as total cysteine, S-adenosyl-homocysteine, cystathionine, and choline. Inflammatory gene expression profiles showed a general downregulation in the setting of elevated plasma homocysteine. HHcy was associated with more and longer microglial processes, but smaller and fewer astrocytes, especially in participants of older age at death. HHcy in older participants was also associated

with occipital cortex microhemorrhages and increased severity of atherosclerosis throughout the cerebral vasculature.

**Conclusions:** Increased plasma homocysteine and older age were associated with the downregulation of inflammatory gene expression markers in association with significant glial and vascular pathology changes. Impaired immune function is a plausible mechanism by which HHcy increases cerebrovascular damage leading to impaired cognitive function.

**KEYWORDS**
Alzheimer's disease, astrocytes, atherosclerosis, hyperhomocysteinemia, microglia, microhemorrhages, neuroinflammation, vascular contributions to cognitive impairment and dementia

## 1 | INTRODUCTION

Vascular contributions to cognitive impairment and dementia (VCID) are a leading cause of dementia that is seen independently or as a comorbid pathology in the setting of Alzheimer's disease (AD). While there is no established treatment to cure VCID, several risk factors that may be therapeutic targets have been identified, with most being risk factors for cardiovascular disease.[1] An underappreciated risk factor for VCID is hyperhomocysteinemia (HHcy). HHcy occurs when plasma total homocysteine (tHcy) levels exceed 14 μmol/L and is well documented as a risk factor for cardiovascular disease and stroke.[2–5] Homocysteine is a non–protein-forming amino acid involved in the metabolism of methionine to cysteine (Figure S1A in supporting information). This metabolic pathway relies on vitamin B6, while conversion from homocysteine back to methionine requires folate and vitamin B12; these three vitamins are essential cofactors for key enzymes, and a diet deficient in these vitamins or impairments in the absorption of these vitamins results in HHcy.[6] Up to 38% of older adults exhibit B vitamin deficiency and one study showed 49% of nursing home patients had a deficiency in vitamin B6.[7,8] While there is data to show that HHcy is associated with cognitive decline, there are limited data assessing the impact of HHcy on neuropathological lesions.

HHcy may affect the brain through various mechanisms. There is strong evidence that HHcy correlates with the severity of atherosclerosis and cardiovascular mortality in patients with coronary artery disease.[9,10] There are also studies investigating the mechanism of HHcy-induced damage in peripheral blood vessels, suggesting a role for oxidative stress, nitric oxide signaling, and endothelial dysfunction.[11,12] Studies show that HHcy is a risk factor for stroke, AD-type dementia, and VCID, and several mouse model studies demonstrate mechanisms by which HHcy leads to these pathologies.[13–15] For example, HHcy increases pro-inflammatory cytokine expression and matrix metalloproteinase 9 activity, which is associated with astrocytic end-foot loss and microhemorrhages.[16,17] Other studies report that HHcy increases tau phosphorylation, decreases cerebral blood flow, and contributes to glutamate neurotoxicity.[18–20]

While there are several proposed mechanisms stemming from these animal data, there is a lack of corresponding human neuropathologic studies to corroborate these findings. Human studies have investigated the association of HHcy with either cognition or neuroimaging changes such as structural brain volume changes and white matter hyperintensities.[21–23] The goal of the present pilot study was to identify neuropathologic changes in human autopsy tissue that are associated with HHcy.

Thirty-one autopsied research volunteers with *ante mortem* homocysteine levels were examined for this pilot study. Levels of homocysteine and related metabolites were measured in both plasma samples taken closest to autopsy and frontal cortex brain tissue. The neuropathologic analysis focused on amyloid and tau pathologies and microgliosis and astrogliosis in the frontal and occipital cortices. Brain indicators of inflammation and angiogenesis were also measured to determine associations with plasma homocysteine levels. Finally, the Human Neuroinflammation NanoString panel was used to determine brain gene expression changes of inflammatory markers associated with high homocysteine levels.

## 2 | METHODS

### 2.1 | Sample selection

To ensure sufficient variability of plasma tHcy, we used *ante mortem* tHcy measurements for our inclusion criteria. Selection of participants with normal tHcy and HHcy were balanced for sex, age at death, cardiovascular risk factors, and neuropathologies present at autopsy. Plasma samples closest to autopsy (range 1–4 years), formalin fixed paraffin embedded, and frozen frontal and occipital cortex samples were obtained through the University of Kentucky Alzheimer's Disease Research Center (UK-ADRC) at the Sanders-Brown Center on Aging. The frontal (Brodmann area 9, corresponding to the middle frontal gyrus) and occipital (Brodmann areas 17/18/19) cortical samples were snap-frozen in liquid nitrogen at the time of autopsy and thereafter stored in a –80°C freezer. Standardized neuropathologic evaluation of atherosclerosis was made using a 0 to 3 grading scale (none, mild, moderate, or severe) at the time of autopsy, based on the observed atherosclerosis in the Circle of

**RESEARCH IN CONTEXT**

1. Systematic Review: The authors used PubMed to review literature on hyperhomocysteinemia and neuropathologic features. While there are considerable data linking hyperhomocysteinemia to radiologic brain changes, there are little data evaluating neuropathologic changes.

2. Interpretation: The findings presented support the extant literature that has demonstrated associations of atherosclerosis with hyperhomocysteinemia and shows considerable glial and vascular changes that have not been previously described. The data suggest a significant interaction effect between age and hyperhomocysteinemia on brain pathology that may be linked to reduced immune function.

3. Future Directions: Given the limited sample size in this pilot study, future studies aimed at evaluating larger numbers of subjects and expanding the characterization of vascular changes related to hyperhomocysteinemia (such as astrocyte end feet) are needed. Increased efforts aimed at understanding the significant downregulation of inflammatory genes due to hyperhomocysteinemia may improve our understanding of the causal pathways whereby hyperhomocysteinemia contributes to vascular contributions to cognitive impairment and dementia.

Willis region. The UK-ADRC recruitment details and pathological assessments performed on autopsy tissue have been previously described.[24]

## 2.2 | Homocysteine metabolites

Total homocysteine and total cysteine: Plasma tHcy was measured by liquid chromatography-tandem mass spectrometry (LC-MS/MS) as previously described.[25] The method was extended to include total cysteine (tCys), Q1/Q3 mass (m/z Cys 122.0/79.1 and d3-Cys 125.1/79.1), declustering potential (31 V), entrance potential (6 V), collision energy (19 V), collision cell exit potential (4 V). To determine tHcy in brain tissue, samples were homogenized in four volumes of 5 mM dithiothreitol and 10μM 2H$_4$-Hcy and incubated on ice for 20 minutes. The homogenized samples were centrifuged at 18,800 × g at 4°C for 10 minutes. Aqueous supernatant was transferred to a micro centrifugal filter unit (Amicon Ultra 0.5 ml, 10 kDa nominal molecular weight limit [NMWL], Millipore) and centrifuged at 18,800 × g at 4°C for 25 minutes. The protein-free filtrate was analyzed for tHcy by LC-MS/MS.[25]

Methylation cycle metabolites: S-adenosyl methionine (SAM), S-adenosyl homocysteine (SAH), methionine, cystathionine, betaine, and choline were measured in plasma and brain tissue by LC-MS/MS

as previously described.[26,27] Briefly, plasma samples were prepared by adding 20 μl of plasma to 180 μl of isotope internal standards in a micro centrifugal filter unit (Amicon Ultra 0.5 ml, 10 kDa NMWL, Millipore) and centrifuged at 18,800 × g at 4°C for 25 minutes. Brain tissue was deproteinized with four volumes of 0.4 M perchloric acid and further diluted 1:10 with isotope internal standards in an aqueous solution. Both plasma and brain tissue extracts were injected into a Nexera LC system (Shimadzu Corporation) coupled to a 5500 QTrap mass spectrometer (SCIEX). Peak detection and quantitation were performed using Analyst 1.7.1 (SCIEX). Two levels of quality control samples were used to monitor the within- and between-day precision of the method. The coefficient of variation (cv) was less than 15% for all metabolites.

## 2.3 | MSD enzyme-linked immunosorbent assay

Frozen frontal and occipital cortex brain regions containing both gray and white matter were pulverized with mortar and pestle over dry ice. Brain tissue was homogenized in 1 ml of Mammalian Protein Extraction Reagent with protease and phosphatase inhibitors and centrifuged at 4°C at 10,000 × g for 15 minutes. The supernatant was collected and using a bicinchoninic acid assay, protein was normalized to 1 mg/ml. Samples were run on MSD's Vascular Injury, Proinflammatory, Cytokine, Chemokine, and Angiogenesis kits according to the manufacturer's instructions (MSD); the only deviation was the Vascular Injury plate was incubated overnight at 4°C. Each plate was read on the MSD Quickplex SQ 120 machine with analysis performed in the MSD Discovery Workbench 4.0 software.

## 2.4 | NanoString and quantitative polymerase chain reaction

RNA was isolated from frozen frontal and occipital cortex containing gray and white matter using the E.Z.N.A. total RNA kit II (Omega Bio-Tek) according to the manufacturer's instructions. RNA quality and quantity was assessed with the Agilent 2100 Bioanalyzer located in the Genomics Core at the University of Kentucky. Samples with a RNA integrity number value lower than seven were excluded from the study (four occipital and two frontal cortex samples excluded). Normalized samples (10 ng/μl) were run on the NanoString Technologies nCounter (also located in the Genomics Core) Human Neuroinflammatory Panel (NanoString).

Quantitative polymerase chain reaction (qPCR) was used to confirm NanoString gene expression changes. Briefly, 100 ng of RNA was reverse transcribed to cDNA using the High-Capacity cDNA kit (Life Technologies) according to the manufacturer's instructions. For qPCR, in each well of a 96-well plate, 1 μl of gene probe, 10 μl of Fast-Taqman reagent, 0.5 μl of cDNA, and 6.5 μl Rnase-free water was loaded and run on the ViiA7 Real-Time PCR System (Applied Biosystems). All genes were normalized to 18 s rRNA and the −ΔΔCt method was used for analysis.

## 2.5 | Immunohistochemistry and histology

Formalin-fixed, paraffin-embedded frontal and occipital cortex brain sections (8 μm thickness) were immunohistochemically stained for amyloid beta (Aβ; 10D5), paired helical filament 1 (PHF-1; phospho-tau), ionized calcium-binding adaptor molecule 1 (IBA-1), and glial fibrillary acidic protein (GFAP). Aβ and PHF-1 were stained by the UK-ADRC Neuropathology Core according to their previously described protocol.[24] Briefly, for IBA-1 (Wako 1:1000 primary, 1:3000 goat anti-rabbit secondary) and GFAP (Dako 1:10,000 primary, 1:5000 goat anti-rabbit secondary), sections were deparaffinized, sodium citrate and 70% formic acid antigen retrieval was performed, and sections were stained as previously described.[28] Sections were also stained for Prussian blue as previously described.[28] IBA-1, GFAP, and Prussian sections were imaged using the Zeiss Axioscan Slide Scanner and analyzed using Indica Lab's HALO imaging software. Aβ and PHF-1 slides were obtained from the UK-ADRC Neuropathology Core, scanned using the Nikon Bio-Pipeline, and analyzed using NIS-Elements.

## 2.6 | Statistical analysis

NanoString analysis: Gene expression values were modeled using linear mixed models with random intercepts and slopes for tissue type within individual to account for the correlation that exists between frontal cortex and occipital samples taken from the same individual. All gene expression values were transformed by the natural logarithm prior to modeling. When estimating the association of HHcy—normal homocysteine (<14 μmol/L) versus HHcy (≥14 μmol/L)—with gene expression, models were adjusted by the sum of all positive control genes and tissue type. The interaction between homocysteine status and tissue type was tested; interactions were only retained if they reached statistical significance. To account for the large number of tests being performed, false discovery rate was applied to the results. Statistical significance was set at q ≤ 0.05 and all tests were two-sided. Missing observations were reported and were excluded on a case-by-case basis. All analyses were done in R programming language, version 3.6.2 (R Foundation for Statistical Computing). All linear mixed models were fit using the lme() function from the R package nlme, version 3.1-142. For the qPCR data, a *t* test was used to determine the significance between normal and HHcy groups.

Homocysteine metabolites, Meso Scale Discovery (MSD), and immunohistochemistry (IHC) analysis: Outliers and influential points were removed from the data set as they had undue influence on the associations. Outliers were removed for each predictor variable using the generalized extreme studentized deviate test (between 0 and 3 outliers removed for each data set). Influential points were determined using delete-1 scaled difference coefficient estimates of the predictor variable to reduce the influence of highly leveraged datapoints (between 0 and 2 influential points removed for each data set). Linear regression models including age at death, sex, plasma tHcy, and the interaction between age and plasma tHcy were performed for all data sets except the atherosclerosis data. Aβ and PHF-1 analysis included the presence of apolipoprotein E ε4 as a covariate in the model. Using the model estimates, the predicted mean value for each outcome at 5 μmol/L plasma tHcy (normal) and 27 μmol/L plasma tHcy (HHcy) for females was generated for the mean age and mean age ± 1 standard deviation to facilitate interpretation of the interaction results. We performed an ordinal logistic regression for atherosclerosis severity and included age, sex, plasma tHcy, and the interaction between plasma tHcy and age.

# 3 | RESULTS

## 3.1 | Homocysteine and metabolites

Sample demographics are shown in Figure 1A. In this pilot study, average plasma tHcy was 15.4 μmol/L, 18 were female (58%), and the average age at death was 85 years. Increased plasma tHcy levels were positively correlated with plasma methionine, cystathionine, total cysteine, SAM, SAH, choline, and betaine and inversely correlated with the SAM/SAH ratio (Figure 1B-J). Only choline and SAM had a significant tHcy and age interaction, where older age with HHcy resulted in higher SAM and choline levels. There was a slight, non-significant, inverse relationship between plasma tHcy and frontal cortex tHcy (Figure 1J, Figure S1). Similar to plasma metabolites, frontal cortex tHcy was inversely associated with the SAM/SAH ratio and positively associated with choline; however, there were no significant age and tHcy interactions (Figure S1B-H). When we compared the frontal cortex metabolites to plasma tHcy, several of the relationships reversed. Choline had an inverse relationship with plasma tHcy in older age, while betaine had a significant positive correlation with plasma tHcy, regardless of age (Figure S2A-G in supporting information).

## 3.2 | Gene and protein expression

In the frontal and occipital cortices combined, the NanoString Human Neuroinflammatory Panel revealed 91 significant gene changes between HHcy (≥ 14μmol/L) and normal plasma tHcy (<14 μmol/L), with the majority of genes being downregulated (Figure 2A, Table S1 in supporting information). qPCR confirmation of genes with a ±25% change showed similar trends as the NanoString results, except for *HCAR2*, which was upregulated on the NanoString analysis but downregulated in qPCR (Figure 2B). *P2RY12* was not significantly changed in the NanoString results and qPCR also confirmed this (Figure 2B).

Analysis of proteins related to inflammation and vascular injury and repair showed a significant age and tHcy interaction for interleukin (IL)5 in both the frontal and occipital cortices, where older age with HHcy led to increased IL5 (Figure 2C,D). IL13 had a slight age and tHcy interaction only in the frontal cortex, where older age with HHcy led to decreased IL13 (Figure 2E,F). IL16 also had a significant age and tHcy interaction where older age with HHcy resulted in decreased IL16 (Table S2 in supporting information lists the *P* values and the predicted values for the remaining proteins).
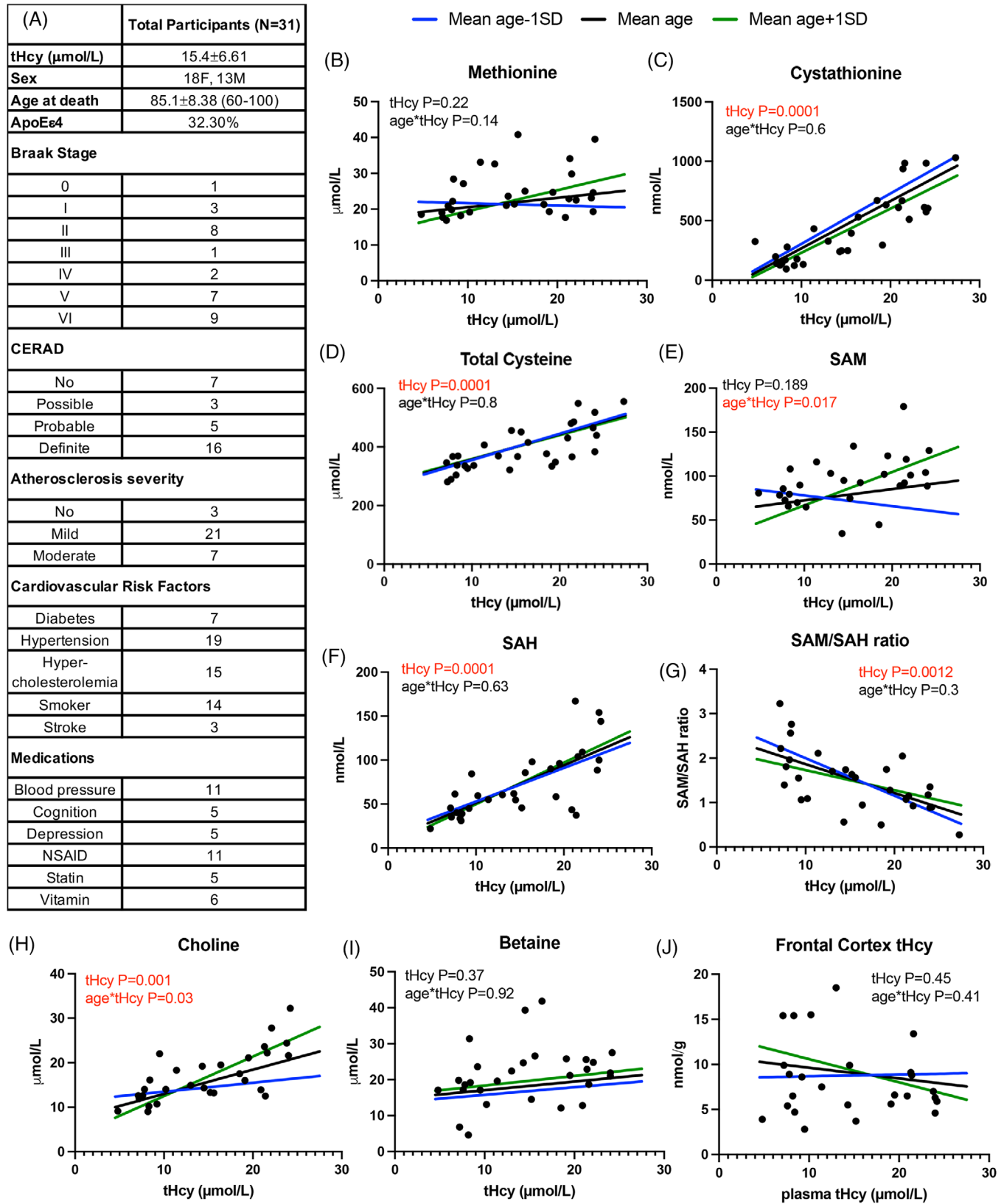
**FIGURE 1** Characterization of participants. A, Table of demographics for the 31 participants included in the study. B–J, Graphs of each homocysteine-related metabolite versus plasma tHcy. The model estimates were used to graph the value of each metabolite at the mean age and mean age ± 1 standard deviation for a female over the raw data points. NSAID, non-steroidal anti-inflammatory; SAH, S-adenosyl homocysteine; SAM, S-adenosyl methionine; SD, standard deviation; tHcy, total homocysteine
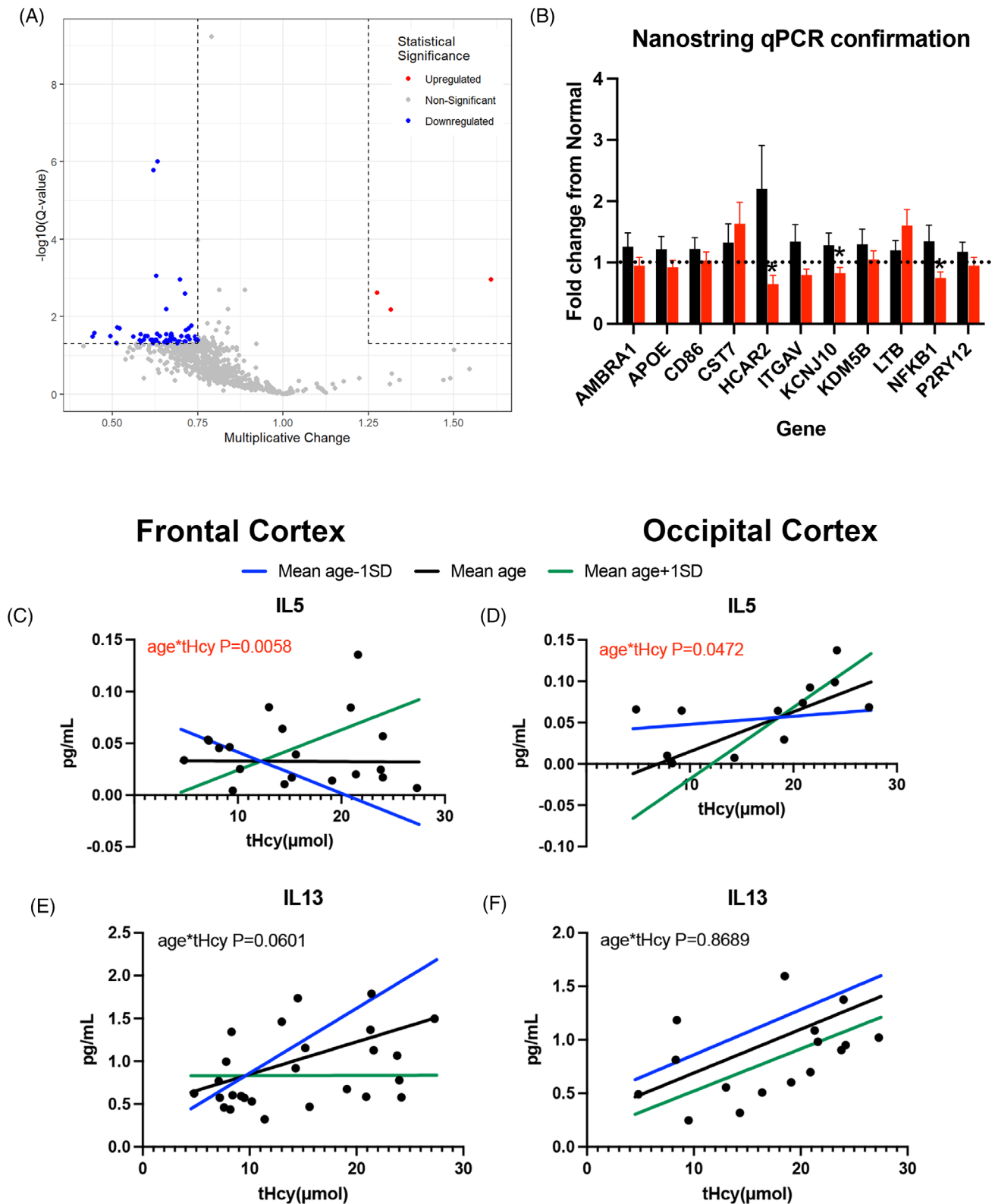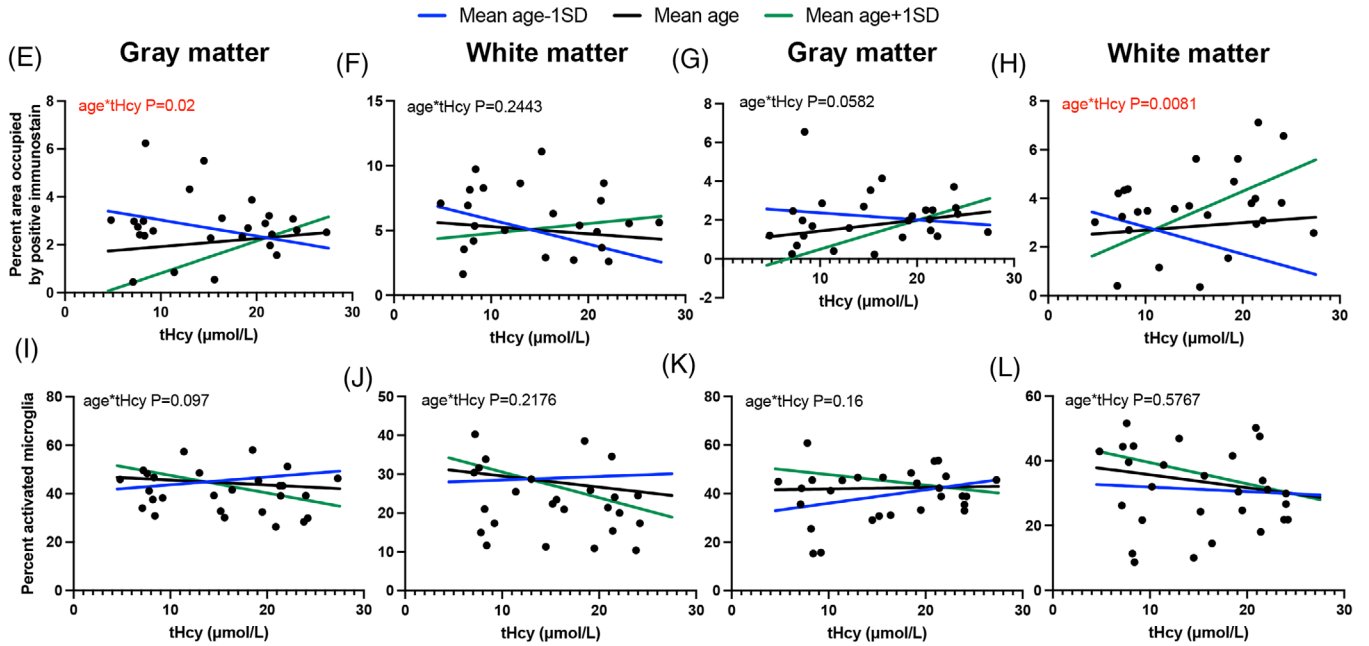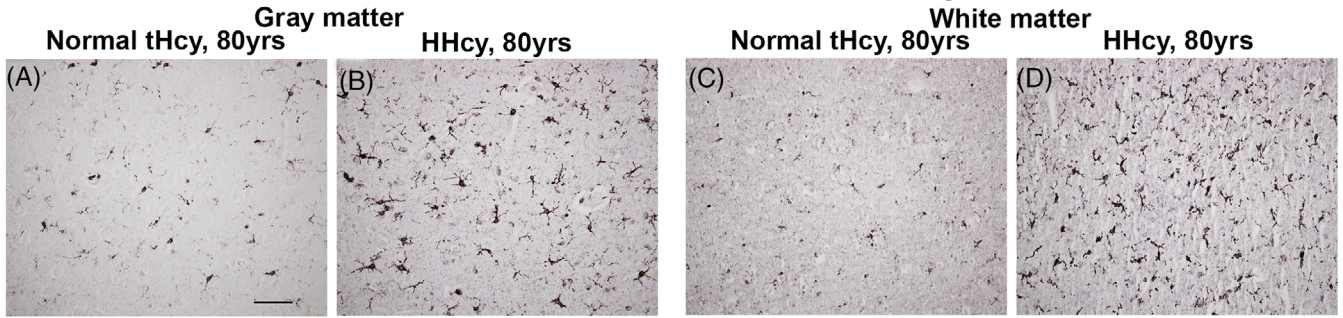
**FIGURE 2** Hyperhomocysteinemia decreases expression of inflammatory-related genes. A, Volcano plot showing the multiplicative change for all genes. B, qPCR for select significant genes. Data are shown as a fold change from normal levels of tHcy. * Indicates $P < 0.05$ compared to normal levels of tHcy. C, IL5 protein expression versus plasma tHcy in the frontal cortex. D, IL5 protein expression versus plasma tHcy in the occipital cortex. E, IL13 protein expression versus plasma tHcy in the frontal cortex. F, IL13 protein expression versus plasma tHcy in the occipital cortex. The model estimates were used to graph the value of each metabolite at the mean age and mean age $\pm$ 1 standard deviation for a female over the raw data points. IL, interleukin; qPCR, quantitative polymerase chain reaction; SD, standard deviation; tHcy, total homocysteine

Figure panels: Frontal Cortex (Gray matter — Normal tHcy, 80yrs (A); HHcy, 80yrs (B)) and Occipital Cortex (White matter — Normal tHcy, 80yrs (C); HHcy, 80yrs (D)). Legend: Mean age-1SD (blue), Mean age (black), Mean age+1SD (green).

(E) Frontal Cortex, Gray matter — age*tHcy P=0.02
(F) Frontal Cortex, White matter — age*tHcy P=0.2443
(G) Occipital Cortex, Gray matter — age*tHcy P=0.0582
(H) Occipital Cortex, White matter — age*tHcy P=0.0081
(I) age*tHcy P=0.097
(J) age*tHcy P=0.2176
(K) age*tHcy P=0.16
(L) age*tHcy P=0.5767

(M)

| | | Frontal Cortex | | | | | | Occipital Cortex | | | | | |
| | | Gray matter | | | White matter | | | Gray matter | | | White matter | | |
| | | Normal | HHcy | P value | Normal | HHcy | P value | Normal | HHcy | P value | Normal | HHcy | P value |
|---|---|---|---|---|---|---|---|---|---|---|---|---|---|
| Microglia count per mm² | Mean age-1SD | 2401.56 | 882.82 | | 4888.77 | 1800.50 | | 1078.87 | 1520.85 | | 2765.77 | 2131.56 | |
| | Mean age | 1116.35 | 1671.24 | 0.0097 | 3945.00 | 3554.50 | 0.245 | 1230.62 | 1582.39 | 0.8857 | 2276.77 | 2961.26 | 0.2246 |
| | Mean age+1SD | -168.86 | 2459.67 | | 3001.24 | 5308.50 | | 1382.38 | 1643.93 | | 1787.78 | 3790.96 | |
| IBA1 percent area | Mean age-1SD | 3.38 | 1.90 | | 6.76 | 2.64 | | 2.55 | 1.76 | | 3.38 | 0.93 | |
| | Mean age | 1.76 | 2.50 | 0.0216 | 5.58 | 4.35 | 0.2443 | 1.15 | 2.40 | 0.0582 | 2.54 | 3.21 | 0.0081 |
| | Mean age+1SD | 0.14 | 3.10 | | 4.40 | 6.06 | | -0.25 | 3.04 | | 1.71 | 5.49 | |
| Avg microglia area (µm²) | Mean age-1SD | 13.30 | 20.83 | | 11.25 | 15.33 | | 11.16 | 16.46 | | 11.39 | 7.68 | |
| | Mean age | 13.66 | 17.15 | 0.0628 | 11.30 | 14.44 | 0.7556 | 11.20 | 15.74 | 0.6762 | 10.64 | 11.60 | 0.0592 |
| | Mean age+1SD | 14.03 | 13.46 | | 11.36 | 13.54 | | 11.24 | 15.01 | | 9.89 | 15.53 | |
| Percent activated | Mean age-1SD | 42.06 | 49.15 | | 28.05 | 30.05 | | 33.25 | 45.47 | | 32.59 | 29.50 | |
| | Mean age | 46.62 | 42.17 | 0.0965 | 30.97 | 24.67 | 0.2176 | 41.62 | 42.96 | 0.1623 | 37.65 | 28.91 | 0.5767 |
| | Mean age+1SD | 51.18 | 35.19 | | 33.89 | 19.28 | | 49.99 | 40.45 | | 42.70 | 28.31 | |
| Avg process area per microglia (µm²) | Mean age-1SD | 21.53 | 24.24 | | 22.61 | 25.70 | | 22.59 | 21.27 | | 23.36 | 21.62 | |
| | Mean age | 21.00 | 23.83 | 0.9397 | 22.14 | 25.57 | 0.861 | 20.37 | 21.95 | 0.112 | 21.24 | 22.81 | 0.1186 |
| | Mean age+1SD | 20.48 | 23.43 | | 21.67 | 25.45 | | 18.15 | 22.62 | | 19.12 | 24.00 | |
| Avg process length per microglia (µm) | Mean age-1SD | 8.68 | 8.43 | | 8.13 | 7.96 | | 8.72 | 7.24 | | 7.76 | 7.25 | |
| | Mean age | 8.60 | 8.62 | 0.464 | 8.13 | 8.15 | 0.6343 | 8.65 | 7.85 | 0.0883 | 7.60 | 7.99 | 0.1528 |
| | Mean age+1SD | 8.51 | 8.80 | | 8.12 | 8.35 | | 8.59 | 8.45 | | 7.44 | 8.72 | |

## 3.3 | Microglia

The effect of plasma tHcy on microglia was evaluated by IHC, which demonstrated that the number of microglia in the gray matter of the frontal cortex were higher with older age with HHcy, but the area of microglia was smaller (Figure 3A,B,E,M). This trend was not significant in the white matter of the frontal cortex (Figure 3F,M). In the white matter of the occipital cortex, older age and HHcy led to an increase in percent area of IBA-1 staining as well as an increase in microglial area (Figure 3C,D,H,M). However, in the gray matter of the occipital cortex, older age with HHcy only led to an increase in percent area (Figure 3G,M).

The microglial activation module on Indica Lab's HALO software allowed us to evaluate activated microglia via process thickness and length. In the gray matter of both the frontal and occipital cortices, older age with tHcy was associated with a decrease in activated microglia (Figure 3I-M). There was an increase in process area and length in the gray and white matter of the occipital cortex, indicating more morphologically different microglia in this region (Figure 3M).

## 3.4 | Astrocytes

In the white matter of both the frontal and occipital cortices, there was a decrease in the number of astrocytes and lower percent area of GFAP labeling with older age and HHcy (Figure 4A-I). There was also a trend toward smaller astrocytes with older age and HHcy in the white matter of both the frontal and occipital cortices (Figure 4I). In the gray matter of the occipital cortex, there was a trend toward fewer, yet larger, astrocytes with older age and HHcy (Figure 4F,I).

## 3.5 | Vascular pathology

The present data demonstrate an increased odds ratio of more severe atherosclerosis with increasing tHcy; however, there was no interaction with age (Figure 5A,B). Prussian blue histology to identify microhemorrhages (mHs), demonstrated a significant increase in the number of mHs with older age and HHcy in the occipital cortex (Figure 5C-E). There was also a trend toward increased size of mHs with older age and higher tHcy in the occipital cortex (Figure 5E). There were no significant associations with the number or size of mHs in the frontal cortex (Figure 5C,E).

## 3.6 | AD pathologies

As HHcy has been shown to be a risk factor for AD,[29] the present study evaluated the association of tHcy on AD neuropathologic changes. There was a trend (not statistically significant) toward increased plaque size with older age and HHcy in both the frontal and occipital cortices (Figure 6A-G). In the frontal cortex there was also a non-significant trend toward increased plaque percent area and total A$\beta$ percent area with older age and HHcy. There was no association with phospho-tau/tangle (PHF-1 immunoreactive) pathology and tHcy (Figure 6G).

## 4 | DISCUSSION

Hyperhomocysteinemia is a risk factor for stroke, VCID, and AD; however, studies linking HHcy to neuropathologic hallmarks of dementia remain lacking. Previous studies have linked HHcy to changes in neuroimaging measures such as brain atrophy, white matter hyperintensities, and infarcts or cognitive performance,[30,31] while only a small number of studies have examined associations of HHcy with dementia-related neuropathologies.[27,32,33] While there are a significant number of animal studies suggesting mechanisms for HHcy-induced damage, there has been no robust human autopsy studies to evaluate these potential mechanisms. The present pilot study evaluated associations of HHcy with pathologic features in 31 autopsied research volunteers who had an *ante mortem* range of plasma tHcy from 4.8 to 27.3 µmol/L. Using fixed and frozen frontal and occipital cortices, the present data demonstrate changes in inflammatory related gene and protein expression, altered microglia and astrocyte number and size, and increased microhemorrhages.

Plasma taken closest to autopsy was evaluated to determine the levels of tHcy and related metabolites. As expected, plasma tHcy–associated metabolites increased with higher plasma tHcy, with a significant age interaction for SAM and choline where older age and HHcy led to an increase in each. While the definition of HHcy is the elevated levels of plasma tHcy, tHcy and metabolites were also measured in frontal cortex. Surprisingly, frontal cortex tHcy did not positively correlate with plasma tHcy and there seemed to be an inverse relationship in older age, although not significant. Because frontal cortex tHcy did not increase proportionally to plasma tHcy, this suggests that the effect of HHcy in the brain may be a downstream effect of a vascular

---

**FIGURE 3** Hyperhomocysteinemia in older age increases microglial staining. Representative images of IBA-1 staining in the gray matter of the frontal cortex of an individual with normal plasma levels of tHcy aged 80 years (A), and an individual with HHcy aged 80 years (B). Representative images of IBA-1 staining in the white matter of the occipital cortex of an individual with normal plasma levels of tHcy aged 80 years (C), and an individual with HHcy aged 80 years (D). Scale bar in (A) = 50 µm. Percent area occupied by positive immunostaining in the gray matter of the frontal cortex (E), white matter of the frontal cortex (F), gray matter of the occipital cortex (G), and the white matter of the occipital cortex (H). The percent of activated microglia in the gray matter of the frontal cortex (I), white matter of the frontal cortex (J), gray matter of the occipital cortex (K), and the white matter of the occipital cortex (L). The model estimates were used to graph the value of each metabolite at the mean age and mean age ± 1 standard deviation for a female over the raw data points. M, Table listing the model estimates for normal (5 µmol/L) and HHcy (27 µmol/L) for the mean age and mean age ± 1 standard deviation for a female and the *P* value for the age and tHcy interaction. HHcy, hyperhomocysteinemia; IBA-1, ionized calcium-binding adaptor molecule 1; SD, standard deviation; tHcy, total homocysteine
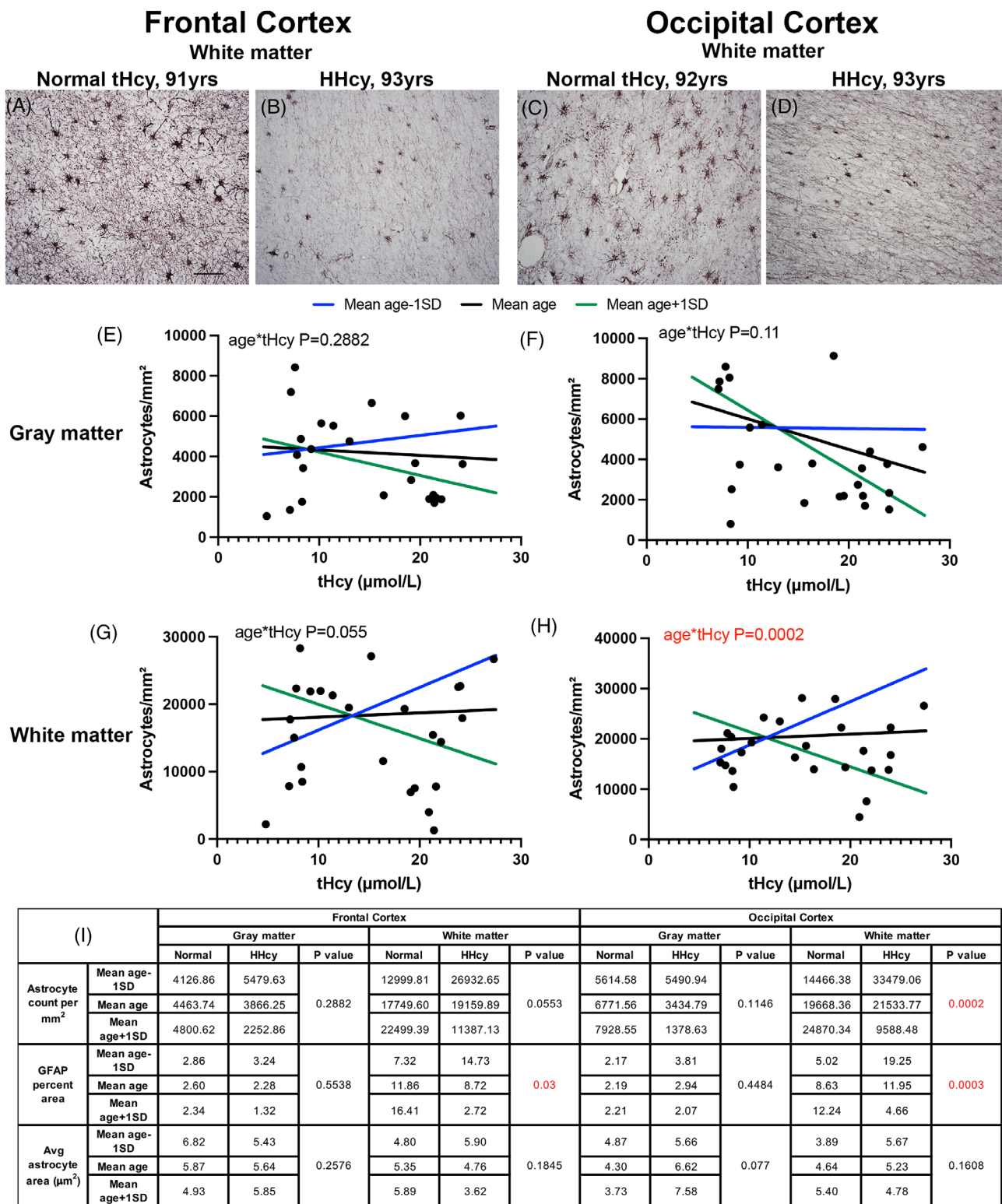
**FIGURE 4** Astrocytes are reduced with HHcy and older age. Representative images of GFAP staining in the white matter of the frontal cortex of an individual with normal plasma levels of tHcy aged 91 years (A), and an individual with HHcy aged 93 years (B). Representative images of GFAP staining in the white matter of the occipital cortex of an individual with normal plasma levels of tHcy aged 92 years (C), and an individual with HHcy aged 93 years (D). Scale bar in (A) = 50 μm. The number of astrocytes/mm² in the gray matter of the frontal cortex (E), gray matter of the occipital cortex (F), white matter of the frontal cortex (G), and the white matter of the occipital cortex (H). The model estimates were used to graph the value of each metabolite at the mean age and mean age ± 1 standard deviation for a female over the raw data points. I, Table listing the model estimates for normal (5 μmol/L) and HHcy (27 μmol/L) for the mean age and mean age ± 1 standard deviation for a female and the *P* value for the age and tHcy interaction. GFAP, glial fibrillary acidic protein; HHcy, hyperhomocysteinemia; SD, standard deviation; tHcy, total homocysteine
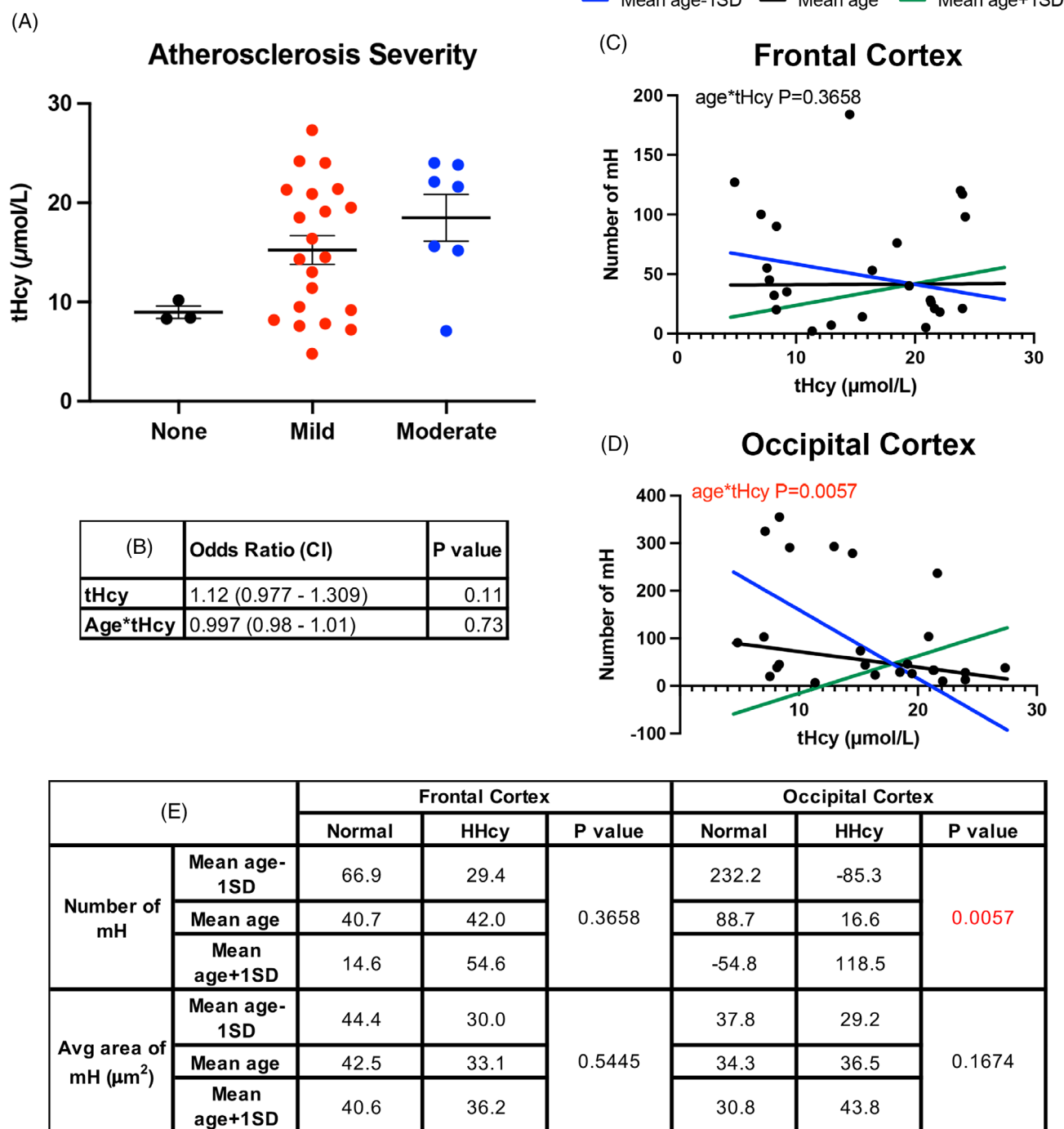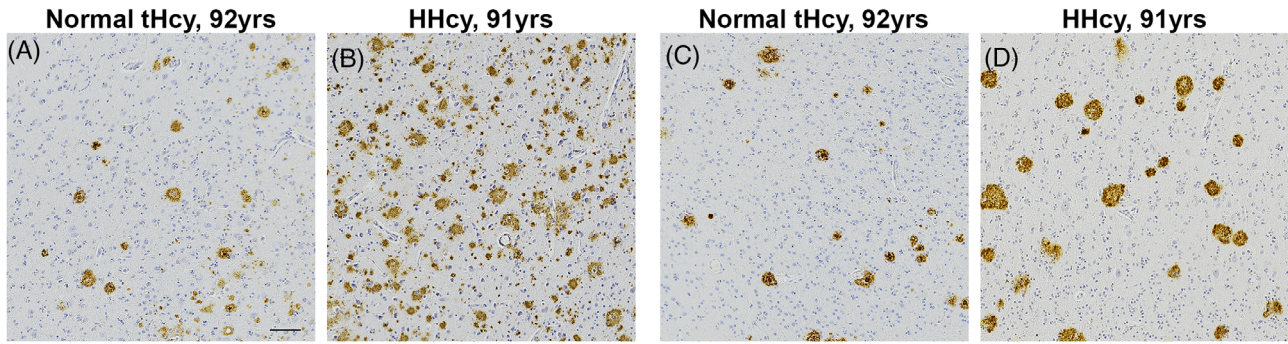
**FIGURE 5** Hyperhomocysteinemia is associated with increased vascular damage. A, Graph of the levels of plasma tHcy grouped by atherosclerosis severity. B, Odds ratio for atherosclerosis severity. Number of mHs in the frontal cortex (C), and occipital cortex (D). The model estimates were used to graph the value of each metabolite at the mean age and mean age ± 1 standard deviation for a female over the raw data points. E, Table listing the model estimates for normal (5 μmol/L) and HHcy (27 μmol/L) for the mean age and mean age ± 1 standard deviation for a female and the *P* value for the age and tHcy interaction. CI, confidence interval; HHcy, hyperhomocysteinemia; SD, standard deviation; tHcy, total homocysteine

response to plasma tHcy. This is the first study we know of to show this phenomenon. Endothelial cells in the cerebrovasculature might be responding to higher homocysteine, producing downstream inflammatory responses in the brain, thus explaining why there are still effects of HHcy seen in our study when frontal cortex tHcy was not increased.

S-adenosyl-methionine is a global methyl donor that contributes a methyl group for DNA methylation. S-adenosyl-homocysteine, an inhibitor of methyltransferases, inhibits SAM.[34] The ratio of SAM/SAH can be used as an indicator of methylation potential, with a lower ratio indicating a lower methylation potential. The present data
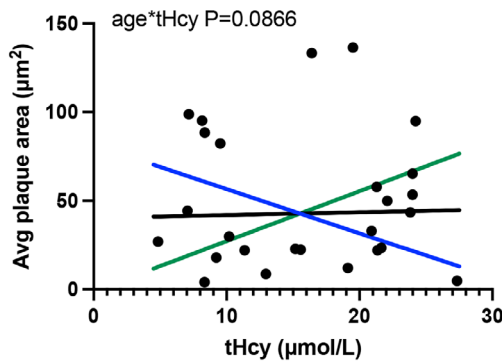
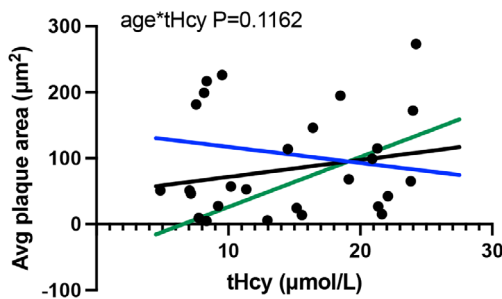**FIGURE 6** A$\beta$ plaque size but not PHF-1 is positively associated with HHcy. Representative images of A$\beta$ staining in the gray matter of the frontal cortex of an individual with normal plasma levels of tHcy aged 92 years (A), and an individual with HHcy aged 91 years (B). Representative images of A$\beta$ staining in the gray matter of the occipital cortex of an individual with normal plasma levels of tHcy aged 92 years (C), and an individual with HHcy aged 91 years (D). Scale bar in (A) = 100 µm. The average A$\beta$ plaque area in the frontal cortex (E) and the occipital cortex (F). The model estimates were used to graph the value of each metabolite at the mean age and mean age ± 1 standard deviation for a female over the raw data points. G, Table listing the model estimates for normal (5 µmol/L) and HHcy (27 µmol/L) for the mean age and mean age ± 1 standard deviation for a female and the P value for the age and tHcy interaction. A$\beta$, amyloid beta; HHcy, hyperhomocysteinemia; PHF-1, paired helical filament 1 (phospho tau); SD, standard deviation; tHcy, total homocysteine

demonstrate a reduced SAM/SAH ratio, suggesting lower methylation levels. While a lower methylation potential would infer higher gene expression, NanoString gene expression data in the present experiment indicate downregulation of the majority of genes in HHcy brain tissue compared to normal plasma tHcy. However, the methyl donor deficiency caused by HHcy could lead to disruption of DNA repair[35,36] and, ultimately, DNA damage, resulting in lower gene expression of inflammatory related genes. Other studies have linked hypomethylation with AD and other neurodegenerative diseases, suggesting a possible mechanism for HHcy-induced damage.[37]

A time course of the HHcy diet in a mouse model has shown there is an initial increase in pro-inflammatory cytokines and microglial staining, followed by a return to basal levels upon continued diet, suggesting resolution of inflammation or microglia becoming senescent.[16,17] The downregulation of inflammatory-related genes examined could be similar to what was seen in this mouse model in which chronic HHcy leads to decreased inflammation. The present data also demonstrate with older age and HHcy, microglia are higher in number but have increased process length and a reduced percent activation, suggesting more homeostatic microglia with higher homocysteine. This also supports the hypothesis that chronic HHcy leads to resolution of inflammation. The increase in IL5, shown to promote microglia proliferation, with older age and HHcy could account for the higher number of microglia observed.[38]

Prior studies in a mouse model of HHcy have shown astrocyte end feet and the cerebrovasculature, crucial components of the neurovascular unit, are significantly degraded. In the present human study, with older age and HHcy, the number of astrocytes is lower in both gray and white matter but higher in gray matter and smaller in white matter, suggesting astrocytes have different responses to HHcy depending on their location. Fewer astrocytes would suggest a loss of astrocyte end feet as well. The data also demonstrate a significant increase in the number and area of microhemorrhages in the occipital cortex, but not the frontal cortex, suggesting different regions of the brain vasculature are more susceptible to HHcy than others. The increased severity of atherosclerosis associated with increased plasma HHcy is consistent with previous studies showing that HHcy increases the risk of atherosclerosis.[9] Taken together, these data demonstrate that HHcy severely impacts the cerebrovasculature, providing a mechanism for how it contributes to VCID pathology.

Hyperhomocysteinemia is also a risk factor for AD and in the present study, a trending but non-significant increased plaque size and total A$\beta$ with older age was associated with HHcy. However, there was no association with PHF-1 or the number of tangles present. The lack of association with PHF-1 in the present study may be an artifact of the small sample size studied.

In summary, the present data demonstrate a significant age and HHcy effect that is associated with downregulation of inflammatory mediators, increased homeostatic microglia, fewer astrocytes, and a disrupted blood–brain barrier. Further studies examining neuropathologic associations of HHcy in human autopsy cohorts are needed to facilitate our understanding of the mechanisms whereby HHcy contributes to VCID and AD. Such revelations may help guide development of much needed future therapeutic interventions for VCID and AD.

## AUTHOR CONTRIBUTION

Peter T. Nelson runs the Neuropathology Core and helped with selection of samples. Gregory A. Jicha runs the Clinical Core and oversees plasma collection. Ela Patel and Shuling X. Fister performed the A$\beta$ and PHF-1 staining. Colin B. Rogers helped with imaging and analysis. Tiffany L. Sudduth ran the MSD plates. Adam J. Dugan and David W. Fardo assisted with NanoString data analysis. Zach Winder and Erin L. Abner assisted in the remaining data analysis. Brandi Wasek and Teodoro Bottiglieri measured homocysteine and the related metabolites. Erica M. Weekman performed data collection, analysis, interpreted the data, and prepared the manuscript. Donna M. Wilcock and Erica M. Weekman conceived of the studies.

## CONFLICTS OF INTEREST

The authors declare they have no conflicts of interest. Author disclosures are available in the supporting information.

## REFERENCES

1. Gorelick PB, Counts SE, Nyenhuis D. Vascular cognitive impairment and dementia. *Biochim Biophys Acta*. 2016;1862(5):860-868. https://doi.org/10.1016/j.bbadis.2015.12.015
2. Beydoun MA, Beydoun HA, Gamaldo AA, Teel A, Zonderman AB, Wang Y. Epidemiologic studies of modifiable factors associated with cognition and dementia: systematic review and meta-analysis. *BMC Public Health*. 2014;14:643. https://doi.org/10.1186/1471-2458-14-643
3. Bostom AG, Rosenberg IH, Silbershatz H, et al. Nonfasting plasma total homocysteine levels and stroke incidence in elderly persons: the Framingham Study. *Ann Intern Med*. 1999;131(5):352-355.
4. Eikelboom JW, Lonn E, Genest J, Jr., Hankey G, Yusuf S. Homocyst(e)ine and cardiovascular disease: a critical review of the epidemiologic evidence. *Ann Intern Med*. 1999;131(5):363-375.
5. Graham IM, Daly LE, Refsum HM, et al. Plasma homocysteine as a risk factor for vascular disease. The European Concerted Action Project. *JAMA*. 1997;277(22):1775-1781.
6. Joosten E, van den Berg A, Riezler R, et al. Metabolic evidence that deficiencies of vitamin B-12 (cobalamin), folate, and vitamin B-6 occur commonly in elderly people. *Am J Clin Nutr*. 1993;58(4):468-476.
7. Hoey L, Strain JJ, McNulty H. Studies of biomarker responses to intervention with vitamin B-12: a systematic review of randomized controlled trials. *Am J Clin Nutr*. 2009;89(6):1981S-1996S. https://doi.org/10.3945/ajcn.2009.27230C
8. Kjeldby IK, Fosnes GS, Ligaarden SC, Farup PG. Vitamin B6 deficiency and diseases in elderly people–a study in nursing homes. *BMC Geriatr*. 2013;13:13. https://doi.org/10.1186/1471-2318-13-13
9. Montalescot G, Ankri A, Chadefaux-Vekemans B, et al. Plasma homocysteine and the extent of atherosclerosis in patients with coronary artery disease. *Int J Cardiol*. 1997;60(3):295-300. https://doi.org/10.1016/s0167-5273(97)00099-5
10. Nygard O, Nordrehaug JE, Refsum H, Ueland PM, Farstad M, Vollset SE. Plasma homocysteine levels and mortality in patients with coronary artery disease. *N Engl J Med*. 1997;337(4):230-236. https://doi.org/10.1056/NEJM199707243370403
11. Esse R, Barroso M, Tavares de Almeida I, Castro R. The contribution of homocysteine metabolism disruption to endothelial dysfunction: state-of-the-art. *Int J Mol Sci*. 2019;20(4):867-891. https://doi.org/10.3390/ijms20040867
12. Ganguly P, Alam SF. Role of homocysteine in the development of cardiovascular disease. *Nutr J*. 2015;14:6. https://doi.org/10.1186/1475-2891-14-6

13. Hofmann MA, Lalla E, Lu Y, et al. Hyperhomocysteinemia enhances vascular inflammation and accelerates atherosclerosis in a murine model. *J Clin Invest*. 2001;107(6):675-83. https://doi.org/10.1172/JCI10588

14. Obeid R, Herrmann W. Mechanisms of homocysteine neurotoxicity in neurodegenerative diseases with special reference to dementia. *FEBS Lett*. 2006;580(13):2994-3005. https://doi.org/10.1016/j.febslet.2006.04.088

15. Tyagi N, Sedoris KC, Steed M, Ovechkin AV, Moshal KS, Tyagi SC. Mechanisms of homocysteine-induced oxidative stress. *Am J Physiol Heart Circ Physiol*. 2005;289(6):H2649-H2656. https://doi.org/10.1152/ajpheart.00548.2005

16. Sudduth TL, Weekman EM, Price BR, et al. Time-course of glial changes in the hyperhomocysteinemia model of vascular cognitive impairment and dementia (VCID). *Neuroscience*. 2017;341:42-51. https://doi.org/10.1016/j.neuroscience.2016.11.024

17. Weekman EM, Sudduth TL, Price BR, et al. Time course of neuropathological events in hyperhomocysteinemic amyloid depositing mice reveals early neuroinflammatory changes that precede amyloid changes and cerebrovascular events. *J Neuroinflam*. 2019;16(1):284. https://doi.org/10.1186/s12974-019-1685-z

18. Braun DJ, Abner E, Bakshi V, et al. Blood flow deficits and cerebrovascular changes in a dietary model of hyperhomocysteinemia. *ASN Neuro*. 2019;11:1-13. https://doi.org/10.1177/1759091419865788

19. Di Meco A, Li JG, Barrero C, Merali S, Pratico D. Elevated levels of brain homocysteine directly modulate the pathological phenotype of a mouse model of tauopathy. *Mol Psychiatry*. 2019;24(11):1696-1706. https://doi.org/10.1038/s41380-018-0062-0

20. Kruman, II, Culmsee C, Chan SL, et al. Homocysteine elicits a DNA damage response in neurons that promotes apoptosis and hypersensitivity to excitotoxicity. *J Neurosci*. 2000;20(18):6920-6926.

21. Lee CC, Hsu SW, Huang CW, et al. Effects of Homocysteine on white matter diffusion parameters in Alzheimer's disease. *BMC Neurol*. 2017;17(1):192. https://doi.org/10.1186/s12883-017-0970-7

22. Rajagopalan P, Hua X, Toga AW, Jack CR, Jr., Weiner MW, Thompson PM. Homocysteine effects on brain volumes mapped in 732 elderly individuals. *Neuroreport*. 2011;22(8):391-395. https://doi.org/10.1097/WNR.0b013e328346bf85

23. Scott TM, Tucker KL, Bhadelia A, et al. Homocysteine and B vitamins relate to brain volume and white-matter changes in geriatric patients with psychiatric disorders. *Am J Geriatr Psychiatry*. 2004;12(6):631-638. https://doi.org/10.1176/appi.ajgp.12.6.631

24. Schmitt FA, Nelson PT, Abner E, et al. University of Kentucky Sanders-Brown healthy brain aging volunteers: donor characteristics, procedures and neuropathology. *Curr Alzheimer Res*. 2012;9(6):724-733. https://doi.org/10.2174/156720512801322591

25. Ducros V, Belva-Besnet H, Casetta B, Favier A. A robust liquid chromatography tandem mass spectrometry method for total plasma homocysteine determination in clinical practice. *Clin Chem Lab Med*. 2006;44(8):987-990. https://doi.org/10.1515/CCLM.2006.178

26. Arning E, Bottiglieri T. Quantitation of S-adenosylmethionine and S-adenosylhomocysteine in plasma using liquid chromatography-electrospray tandem mass spectrometry. *Methods Mol Biol*. 2016;1378:255-262. https://doi.org/10.1007/978-1-4939-3182-8_27

27. Kalecky K, Ashcraft P, Bottiglieri T. One-carbon metabolism in Alzheimer's disease and Parkinson's disease brain tissue. *Nutrients*. 2022;14(3):599-617. https://doi.org/10.3390/nu14030599

28. Seaks CE, Weekman EM, Sudduth TL, et al. Apolipoprotein E epsilon4/4 genotype limits response to dietary induction of hyperhomocysteinemia and resulting inflammatory signaling. *J Cereb Blood Flow Metab*. 2022;42(5):771-787. https://doi.org/10.1177/0271678%D7;211069006

29. Seshadri S, Beiser A, Selhub J, et al. Plasma homocysteine as a risk factor for dementia and Alzheimer's disease. *N Engl J Med*. 2002;346(7):476-483. https://doi.org/10.1056/NEJMoa011613

30. Kloppenborg RP, Nederkoorn PJ, van der Graaf Y, Geerlings MI. Homocysteine and cerebral small vessel disease in patients with symptomatic atherosclerotic disease. The SMART-MR study. *Atherosclerosis*. 2011;216(2):461-466. https://doi.org/10.1016/j.atherosclerosis.2011.02.027

31. Seshadri S, Wolf PA, Beiser AS, et al. Association of plasma total homocysteine levels with subclinical brain injury: cerebral volumes, white matter hyperintensity, and silent brain infarcts at volumetric magnetic resonance imaging in the Framingham Offspring Study. *Arch Neurol*. 2008;65(5):642-649. https://doi.org/10.1001/archneur.65.5.642

32. Hooshmand B, Polvikoski T, Kivipelto M, et al. Plasma homocysteine, Alzheimer and cerebrovascular pathology: a population-based autopsy study. *Brain*. 2013;136(Pt 9):2707-2716. https://doi.org/10.1093/brain/awt206

33. Kalecky K, German DC, Montillo AA, Bottiglieri T. Targeted metabolomic analysis in Alzheimer's disease plasma and brain tissue in Non-Hispanic Whites. *J Alzheimers Dis*. 2022;86(4):1875-1895. https://doi.org/10.3233/JAD-215448

34. Hoffman DR, Cornatzer WE, Duerre JA. Relationship between tissue levels of S-adenosylmethionine, S-adenylhomocysteine, and transmethylation reactions. *Can J Biochem*. 1979;57(1):56-65. https://doi.org/10.1139/o79-007

35. Chen RZ, Pettersson U, Beard C, Jackson-Grusby L, Jaenisch R. DNA hypomethylation leads to elevated mutation rates. *Nature*. 1998;395(6697):89-93. https://doi.org/10.1038/25779

36. Sheaffer KL, Elliott EN, Kaestner KH. DNA hypomethylation contributes to genomic instability and intestinal cancer initiation. *Cancer Prev Res (Phila)*. 2016;9(7):534-546. https://doi.org/10.1158/1940-6207.CAPR-15-0349

37. Nikolac Perkovic M, Videtic Paska A, Konjevod M, et al. Epigenetics of Alzheimer's disease. *Biomolecules*. 2021;11(2):195-233. https://doi.org/10.3390/biom11020195

38. Liva SM, de Vellis J. IL-5 induces proliferation and activation of microglia via an unknown receptor. *Neurochem Res*. 2001;26(6):629-637. https://doi.org/10.1023/a:1010983119125

## SUPPORTING INFORMATION

Additional supporting information can be found online in the Supporting Information section at the end of this article.